

RESEARCH

Open Access



Antiproliferation effects of nanophytosome-loaded phenolic compounds from fruit of *Juniperus polycarpus* against breast cancer in mice model: synthesis, characterization and therapeutic effects

Soheila Moeini¹, Ehsan Karimi^{1*} and Ehsan Oskoueian^{2*}

*Correspondence:
ehsankarimi@mshdiau.ac.ir;
e.oskoueian@gmail.com

¹Department of Biology,
Mashhad Branch, Islamic Azad
University, Mashhad, Iran

²Department of Research
and Development, Arka
Industrial Cluster, Mashhad, Iran

Abstract

Background: This research was performed to synthesize nanophytosome-loaded high phenolic fraction (HPF) from *Juniperus polycarpus* fruit extract and investigate its antiproliferation effects against breast cancer in mice model.

Results: The nanophytosome-loaded HPF from *Juniperus polycarpus* fruit extract was synthesized. The mice trial was conducted to determine the possible toxic effects of the synthesized nanophytosomes. The anticancer, pro-apoptotic, and antioxidative activities of the nanophytosomes were determined. The nanophytosome-loaded HPF had a spherical structure with a size of 176 nm and a polydispersity index coefficient of 0.24. The in vivo study manifested that nanophytosome-loaded HPF significantly improved weight gain and food intake compared to the negative control group ($p < 0.05$). The nanophytosome-loaded HPF significantly enhanced the expression of bax (3.4-fold) and caspase-3 (2.7-fold) genes, but reduced bcl2 (3.6-fold) gene expression in tumor cells. The average tumor size was significantly decreased in mice treated with nanophytosome-loaded HPF ($p < 0.05$). The expression of GPX (2.3-fold) and SOD (2.7-fold) antioxidants in the liver of mice supplemented with nanophytosome-loaded HPF was significantly developed compared to the negative control ($p < 0.05$). The nanophytosome-loaded HPF did not show toxicity on normal cells.

Conclusion: Our results indicated that nanophytosome-loaded HPF might be a potential anticancer agent for the breast cancer treatment.

Keywords: Drug delivery, Phytogetic, Phytosome, Phenolic compound

Background

Breast cancer is the second most common cancer in the world and the most common cancer among women worldwide (Dumitrescu and Cotarla 2005). It is also the second most common cause of cancer death among women globally (Momenimovahed and Salehiniya 2019). In 2012, 1.67 million new breast cancer cases were identified



© The Author(s) 2022. **Open Access** This article is licensed under a Creative Commons Attribution 4.0 International License, which permits use, sharing, adaptation, distribution and reproduction in any medium or format, as long as you give appropriate credit to the original author(s) and the source, provide a link to the Creative Commons licence, and indicate if changes were made. The images or other third party material in this article are included in the article's Creative Commons licence, unless indicated otherwise in a credit line to the material. If material is not included in the article's Creative Commons licence and your intended use is not permitted by statutory regulation or exceeds the permitted use, you will need to obtain permission directly from the copyright holder. To view a copy of this licence, visit <http://creativecommons.org/licenses/by/4.0/>. The Creative Commons Public Domain Dedication waiver (<http://creativecommons.org/publicdomain/zero/1.0/>) applies to the data made available in this article, unless otherwise stated in a credit line to the data.

worldwide, accounting for 25% of all cancers (Momenimovahed and Salehiniya 2019). In recent years, some limitations, such as the high cost and side effects caused by synthetic chemical anticancer drugs, have forced scientists to search for new anticancer substances (Enyew et al. 2014).

Plant secondary metabolites are rich sources of bioactive constituents utilized in the pharmaceutical industry, meal additives, flavors, and other industrial materials. These substances are also known to play an important role in adapting plants to their environment (Selvakumar et al. 2020). Bioactive natural compounds are employed to develop cheaper, safer, and more effective anti-inflammatory and anticancer drugs (Wangchuk 2018). Among such natural chemical compounds, essential oils and phenolic and flavonoid components are proven beneficial antioxidants, antitumor, and anticancer agents. These compounds comprise several pharmacological properties that could prevent the creation of ROS and DNA damage and induce apoptosis through the caspase, P53, and other involved genes (Roleira et al. 2015). Plant secondary metabolites are regarded as potential chemopreventive agents which block cancer recurrence and prevent the development of invasive cancer. For these reasons, the global demand for herbal medicines is considerably increased (Beatrice 2015).

Various technologies are adopted to promote and extract bioactive molecules in medicinal plants. Plant-derived bioactive compounds are used as medicines, herbal chemicals, flavors, fragrances, food additives, and pesticides (Niazian 2019). However, solubility, limited availability and absorption capacity and toxicity damage are significant obstacles in applying herbal medicine (Niazian 2019). Fortunately, recent advances in nanotechnology provide excellent conditions to minimize these barriers in herbal medicine. For example, nanotechnology provides powerful systems for effective drug delivery through nanoparticles and nanostructures, e.g., liposomes, phytosomes, lipid transporter nanostructures, and solid lipid nanoparticles that carry anticancer components such as rutin, anthocyanins, catechins, and silymarin (Babazadeh et al. 2017, 2016).

Nanophytosomes are now considered valuable carriers of drugs and plant nutrients, and plant extracts (Babazadeh et al. 2018). The nanophytosome formulation is an ideal carrier for drug delivery because its nuclei are composed of phospholipids and cholesterol, similar to biological membranes (Sindhumol et al. 2010; Kulkarni 2011; Ghanbarzadeh et al. 2016). Nano-based drug delivery system has advantages over traditional drug delivery systems. The nano-based systems have more efficient drug distribution, better-controlled drug release, and directly target cancer tissues with more excellent permeability and long-lasting effect (Weinberg et al. 2005). In addition, nanophytosomes have biologically neutral structures and produce less immunogenic reactions.

Juniperus is one of the chief genera of the Cupressaceae family. It is estimated that 70 species of Juniperus are dispersed all over the world (Topçu et al. 1999). Juniperus is indicated in Iran by five species. Juniperus excelsa is divided into two subspecies including *J. excelsa* M. B subsp. *Excelsa* and *J. excelsa* M. B subsp. *Polycarpus*. (*Juniperus polycarpus*, generally known as Persian juniper or “Ors” and is a dioecious tree up to 6–7 m high or a low shrub with dense head (Emami et al. 2011), additionally broadly dispensed in different areas such as south-east Arabia, Iran, Caucasus, Baluchistan, Afghanistan, north-west Himalaya (Tutin et al. 1980). The *J. excelsa* subsp. *polycarpus* is a medicinal plant used traditionally to cure different types of illness in animals and humans like

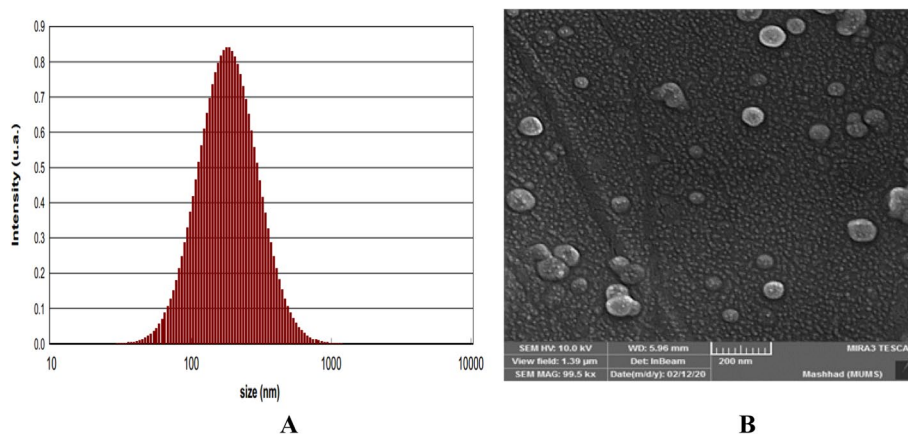


Fig. 1 Characteristic features of nanophytosomes

Table 1 Physical characteristics of nanophytosome-loaded high phenolic-rich fraction from *Juniperus polycarpus* fruit

Particle size (nm)	Polydispersity index (PDI)	Zeta potential (mV)
176.34	0.24	-53.8

asthma and earache. It has been articulated that the extracted compounds of *J. excelsa* subsp. *polycarpus* possess antimicrobial, antifungal, and antioxidant activities (Moein et al. 2010; Hosseinihashemi et al. 2017; Mohiti-Asli and Ghanaatparast-Rashti 2018). This study was performed to synthesize the nanophytosome-loaded phenolic compounds from the *Juniperus polycarpus* tree's fruit and evaluate its anticancer potential against breast cancer in Balb/c mice.

Results

Fractionation and total phenolic content

The different polarity fractions from *Juniperus polycarpus* fruit in different quantities were obtained. The highest total phenolic compounds (TPC) was detected in ethyl acetate fraction 298.4 ± 2.16 followed by n-butanol (127.3 ± 5.76) > water (63.4 ± 8.59) > chloroform (14.6 ± 8.38) > hexane (11.6 ± 5.96) mg GAE/g DW of extract, respectively. The ethyl acetate fraction possessed the highest concentration of phenolic compounds hence named a high phenolic-rich fraction (HPF) and was used for further experiments.

Characterization of phytosomes

The fractionation results indicated the ethyl acetate fraction as the highest concentration of phenolic compounds; hence the synthesis of phytosomes was performed using this fraction. Figure 1 demonstrates physical characteristics of nanophytosomes, including Z-average particle size (A), zeta potential (B), and FESEM image (C). The zeta potential and particle size of nano-phytosome-loaded by HPF were -53.8 mV and 176.34 nm, respectively (Table 1). The polydispersity index, which is the particle size distribution index for the nanophytosome of HPF, was found to be 0.24, which is in the range of the most suitable size for medical and pharmaceutical applications. The FESEM analysis

Table 2 Phenolic compounds present in the nanophytosome-loaded high phenolic-rich fraction from *Juniperus polycarpus* fruit

Phenolic compounds ($\mu\text{g/g}$)		
Syringic acid 171.8 \pm 2.4	Naringin 509.5 \pm 4.5	Ferulic acid 713.5 \pm 3.8
Ellagic acid 923 \pm 5.3	Cinnamic acid 87.2 \pm 2.1	Salicylic acid 622.5 \pm 2.5

Table 3 The averages of mice body weight changes and food intake during experiment receiving different concentrations of high phenolic-rich fraction from *Juniperus polycarpus* fruit

Average	M1	M2	M3	M4	SEM
Average daily weight gain (mg)	22.3 ^d	37.5 ^c	67.3 ^a	60.2 ^b	4.59
Average daily food intake (g)	2.1 ^c	2.6 ^b	3.2 ^a	2.9 ^a	0.17

M1 (Control), M2 mice receiving HPF (25 mg TPC/kg/BW), M3 mice receiving HPF (50 mg TPC/kg/BW), and M4 mice receiving HPF (100 mg TPC/kg/BW), different letters (a, b, c, d) in the same row represent significant difference ($p < 0.05$); the analysis was performed in triplicates

confirmed that nanosize of phytosomes-loaded HPE, which were morphologically spherical and exhibited almost the same size, confirming the particle size results.

HPLC analysis

The phenolic compounds profiling of nanophytosome-loaded HPF indicated different types of bioactive compounds (Table 2). The HPLC analysis revealed the presence of ellagic acid and ferulic acid as the major phenolic compounds with respective values of 923 and 713.5 μg .

Toxicity assay

The average daily weight gain and daily food intake in each treatment are shown in Table 3. The average daily weight gain and daily food intake showed significant ($p < 0.05$) differences between groups. The increase in the HPF concentration up to 50 mg/kg BW significantly ($p < 0.05$) improved the average daily weight gain and food intake as compared to the control. However, the application of HPF above 50 mg/kg BW showed significant ($p < 0.05$) detrimental effects on weight gain and food intake.

The liver enzymes (ALP, ALT, and AST) and MDA as lipid peroxidation values are considered biomarkers of hepatic damage and hepatotoxicity. The increase in HPF concentration up to 50 mg TPC/kg/BW did not alter these parameters significantly ($p > 0.05$) (Table 4). While the increase in the concentration of HPF above 50 mg TPC/kg/BW significantly ($p < 0.05$) impaired the liver enzymes and lipid peroxidation in the liver, which confirms the hepatic damage.

Antiproliferative activity

In the toxicity assay, we found that the concentration of 50 mg TPC/kg/BW of high phenolic-rich fraction from *Juniperus polycarpus* fruit is not detrimental and toxic for the mice. Hence the antiproliferative activity of the HPF was performed using 50 mg

Table 4 The results of liver enzymes analysis and lipid peroxidation in the liver tissue of mice receiving different concentrations of high phenolic-rich fraction from *Juniperus polycarpus* fruit

Parameters	M1	M2	M3	M4	SEM
ALT (IU/L)	154 ^b	153 ^b	165 ^b	188 ^a	7.63
AST (IU/L)	62 ^b	64 ^b	68 ^b	71 ^a	4.9
ALP (IU/L)	561 ^b	559 ^b	569 ^b	602 ^a	11.6
MDA* (%)	100.0 ^a	91.4 ^b	79.6 ^c	96.8 ^b	7.68

M1 (Control), M2 mice receiving HPF (25 mg TPC/kg/BW), M3 mice receiving HPF (50 mg TPC/kg/BW), and M4 mice receiving HPF (100 mg TPC/kg/BW), different letters (a, b, c, d) in the same row represent significant difference ($p < 0.05$), the analysis was performed in triplicates

* Expressed as malondialdehyde changes relative to the control group

HPF/Kg/BW. The results of antiproliferative activities are presented in Table 5. The results indicated that nanophytosome-loaded HPF at 50 mg TPC/kg/BW improved the average daily weight gain and food intake significantly ($p < 0.05$) compared to the control group. In addition, the nanophytosome-loaded HPF appeared to be more potent ($p < 0.05$) in improving the average daily weight gain and food intake in the mice compared to the mice receiving un-capsulated HPF at the similar dose. The tamoxifen as an antiproliferative drug at the concentration of 0.4 mg/kg/BW similar dose to the clinical dose in humans impaired ($p < 0.05$) the values for the average daily weight gain and food intake compared to the control group.

The results of liver enzymes (ALP, ALT, and AST) and MDA as lipid peroxidation value are considered as biomarkers of hepatocyte damage, and hepatotoxicity are shown in Table 6. These results showed that liver enzymes (ALP, ALT, and AST) and MDA were improved upon treatment of mice with HPF and nanophytosome-loaded HPF. However, the effectiveness of nanophytosome-loaded HPF was more prominent

Table 5 The averages of body weight changes and food intake in the TUBO tumor-bearing mice during experiment receiving different treatments

Average	T1	T2	T3	T4	SEM
Average daily weight gain (mg)	63.4 ^c	78.9 ^b	94.2 ^a	42.6 ^d	5.43
Average daily food intake (g)	2.85 ^c	3.01 ^b	3.16 ^a	2.69 ^d	0.06

Control (T1); mice receiving HPF (50 mg TPC/Kg/BW) (T2); mice were receiving nanophytosome-loaded HPF (50 mg TPC/Kg/BW) (T3); and mice receiving tamoxifen (0.4 mg/kg/BW similar dose to the clinical dose in humans) as an antiproliferative drug (T4). Different letters (a, b, c, d) in the same row represent significant difference ($p < 0.05$); the analysis was performed in triplicates

Table 6 The results of liver enzymes analysis and lipid peroxidation in the liver tissue of TUBO tumor-bearing mice during experiment receiving different treatments

Parameters	T1	T2	T3	T4	SEM
ALT (IU/L)	177 ^a	145 ^b	123 ^c	125 ^c	8.72
AST (IU/L)	63 ^a	50 ^b	46 ^b	52 ^b	4.18
ALP (IU/L)	789 ^a	466 ^b	312 ^c	455 ^b	51.7
MDA* (%)	100.0 ^a	92.4 ^b	84.7 ^c	94.6 ^b	2.47

Control (T1); mice receiving HPF (50 mg TPC/Kg/BW) (T2); mice were receiving nanophytosome-loaded HPF (50 mg TPC/Kg/BW) (T3); and mice receiving tamoxifen (0.4 mg/kg/BW similar dose to the clinical dose in humans) as an antiproliferative drug (T4). Different letters (a, b, c, d) in the same row represent significant difference ($p < 0.05$). The analysis was performed in triplicates

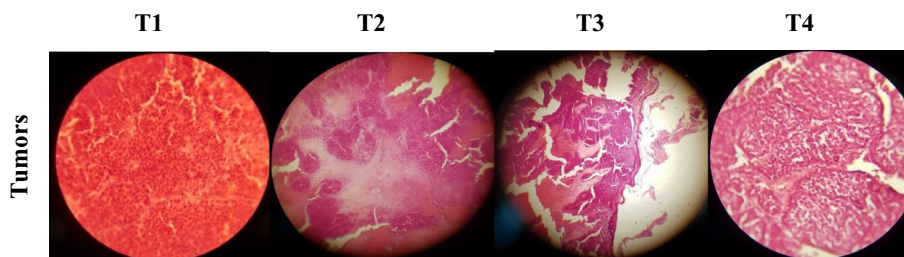


Fig. 2 The histopathological changes in the TUBO tumor-bearing mice during experiments receiving different treatments. Control (T1); mice receiving HPF (50 mg TPC/Kg/BW) (T2); mice were receiving nanophytosome-loaded HPF (50 mg TPC/kg/BW) (T3); and mice receiving tamoxifen (0.4 mg/kg/BW similar dose to the clinical dose in humans) as an antiproliferative drug (T4)

Table 7 The size of tumor upon 28 days in TUBO tumor-bearing mice during experiment receiving different treatments

Tumor	T1	T2	T3	T4	SEM
Weight (g)	3.4 ^a	2.94 ^b	2.63 ^c	1.59 ^d	0.16
Size (mm)	26.5 ^a	25.2 ^b	22.5 ^c	19.6 ^d	0.38

Control (T1); mice receiving HPF (50 mg TPC/kg/BW) (T2); mice were receiving nanophytosome-loaded HPF (50 mg TPC/Kg/BW) (T3); and mice receiving tamoxifen (0.4 mg/kg/BW similar dose to the clinical dose in humans) as an antiproliferative drug (T4). Different letters (a, b, c, d) in the same row represent significant difference ($p < 0.05$). The analyses were performed in triplicates

($p < 0.05$) in alleviating these parameters compared to the HPF in the treated mice. However, the tamoxifen could suppress ($p < 0.05$) the liver enzymes and lipid peroxidation, the improvement was not comparable to that of un-encapsulated and nanophytosome encapsulated HPF.

Tumor characteristics

The histopathological changes of tumors in each group are depicted in Fig. 2. In the T1 group, tumor areas were solid, with high cell density, without glandular structure. In the T2 group, cell density decreased, but differentiation did not change significantly. However, necrosis was more widespread than in the negative control, indicating the lethal effect of the HPF on cancer cells. Similarly, in the T3 group, cell density decreased, and differentiation did not show a significant change. However, necrosis has become more widespread than in the negative control and T2 groups, indicating that the nanophytosome-loaded HPF has a more lethal effect on necrotic cancer cells than the un-encapsulated HPF. In the T4 group, cell density decreased compared to the negative control, but cell differentiation increased, which seems to be due to cell apoptosis caused by the effect of tamoxifen. Glandular structures were formed, and the tumor was changed from the solid form in different areas, directly related to tamoxifen’s antiproliferative effects.

A significant difference was observed in the mean of tumor weight and size between groups ($p < 0.05$). The control group collectively showed significantly higher tumor weight and larger size than other groups ($p < 0.05$; Table 7), revealing the antiproliferative effects of HPF and nanophytosome-loaded HPF. The weight and size of the tumor revealed that the nanophytosome-loaded HPF possessed more antiproliferative effects



Fig. 3 Comparison of the tumor size in TUBO tumor-bearing mice during experiments receiving different treatments. Control (T1); mice receiving HPF (50 mg TPC/Kg/BW) (T2); mice were receiving nanophytosome-loaded HPF (50 mg TPC/kg/BW) (T3); and mice receiving tamoxifen (0.4 mg/kg/BW similar dose to the clinical dose in humans) as an antiproliferative drug (T4)

Table 8 Morphometric analysis of jejunum in TUBO tumor-bearing mice during experiments receiving different treatments

Treatment	T1	T2	T3	T4	SEM
Villus height (μm)	271.2 ^c	325.3 ^b	376.6 ^a	251.7 ^c	12.65
Villus width (μm)	81.1 ^c	86.4 ^b	94.6 ^a	77.7 ^c	9.17
Crypt depth (μm)	138.6 ^a	115.7 ^b	105.6 ^c	134.5 ^a	7.89
Goblet cells (μm)	3.5 ^b	3.8 ^a	4.1 ^a	4.9 ^a	0.71

Control (T1); mice receiving HPF (50 mg TPC/kg/BW) (T2); mice were receiving nanophytosome-loaded HPF (50 mg TPC/kg/BW) (T3); and mice receiving tamoxifen (0.4 mg/kg/BW similar dose to the clinical dose in humans) as an antiproliferative drug (T4)

Different letters (a, b, c, d) in the same row represent significant difference ($p < 0.05$)

($p < 0.05$) than the un-encapsulated HPF. The T4 group exhibited the lowest mean tumor weight and size, followed by T3 and T2 groups (Table 7 and Fig. 3).

Morphometric analysis of jejunum

Morphometric analysis of jejunum in different groups is shown in Table 8. There was a significant difference in the mean size of villus height and width and crypt depth and goblet cells between groups ($p < 0.05$). These findings showed that the oral administration of HPF and nanophytosome-loaded HPF notably ($p < 0.05$) improved the villus height, villus width, number of goblet cells, and decreased the crypt depth. These outcomes followed an earlier study (Mohiti-Asli and Ghanaatparast-Rashti 2018) that informed that adding phenolic compounds in the animal diet improved the small intestine's morphometric parameters. Afterward, the intestinal absorption of nutrients is increased. Hence, the significant increase in the food intake and average daily weight gain of mice upon oral administration of fruit extract should enhance the morphology of the jejunum and enlargement the absorption of nutrients.

Table 9 The changes in the expression of apoptosis-related genes in the TUBO tumor in the mice receiving different treatments

Genes	Gene expression (fold changes)				S.E.M
	T1	T2	T3	T4	
Up-regulated genes					
Bax	1.0 ^d	2.6 ^c	3.4 ^b	4.8 ^a	0.09
Caspase-3	1.0 ^d	1.9 ^c	2.7 ^b	3.9 ^a	0.11
Down-regulated genes					
Bcl2	1.0 ^d	2.3 ^c	3.6 ^b	5.2 ^a	0.08

Control (T1); mice receiving HPF (50 mg TPC/Kg/BW) (T2); mice were receiving nanophytosome-loaded HPF (50 mg TPC/Kg/BW) (T3) and mice receiving tamoxifen (0.4 mg/kg/BW similar dose to the clinical dose in humans) as an antiproliferative drug (T4). Different letters (a, b, c, d) in the same row represent significant difference ($p < 0.05$). The analysis was performed in triplicates

Table 10 The changes in the expression of antioxidant-related genes in mice liver receiving different treatments

Genes	Gene expression (fold changes)				S.E.M
	T1	T2	T3	T4	
SOD	1.0 ^c	1.9 ^b	2.7 ^a	2.1 ^b	0.11
GPX	1.0 ^d	1.4 ^c	2.3 ^a	1.8 ^b	0.09

Control (T1); mice receiving HPF (50 mg TPC/kg/BW) (T2); mice were receiving nanophytosome-loaded HPF (50 mg TPC/kg/BW) (T3); and mice receiving tamoxifen (0.4 mg/kg/BW similar dose to the clinical dose in humans) as an antiproliferative drug (T4); different letters (a, b, c, d) in the same row represent significant difference ($p < 0.05$); the analysis was performed in triplicates

Gene expression analysis

Gene expression analysis showed a significant difference in the expression pattern of bax, bcl2, and caspase-3 between groups ($p < 0.001$; Table 9). Mice treated with HPF, nanophytosome-loaded HPF, and tamoxifen showed significant down-regulation of bcl2 ($p < 0.001$) and overexpression of bax and caspase-3 genes as compared to the control group ($p < 0.01$). However, the highest increase in bax and caspase-3 gene expression was found in the T4 group, followed by T3 and T2 groups. Compared to the control group, tamoxifen caused a significant increase in bax and caspase-3 expression by 4.8-fold and 3.9-fold, respectively ($p < 0.001$). In contrast, mice treated with tamoxifen showed a significant decrease in bcl2 expression by 5.2-fold rather than animals in the control group ($p < 0.001$; Table 9). Similar to tamoxifen, nano-phytosome-loaded extract significantly enhanced bax (3.4-fold) and caspase-3 (2.7-fold) expression but decreased bcl2 expression by 3.6-fold ($p < 0.05$).

A significant difference was seen in the expression pattern of SOD and GPX Genes between groups ($p < 0.001$; Table 10). Mice treated with HPF, nanophytosome-loaded HPF, and tamoxifen showed significant overexpression of SOD and GPX compared to the control group ($p < 0.05$). The highest increase in SOD and GPX gene expression was found in the T3 group, followed by T4 and T2 groups. Compared to the control group, nanophytosome-loaded HPF caused a significant increase in SOD and GPX expression by 2.7-fold and 2.3-fold, respectively ($p < 0.001$).

Discussion

This research considered the effect of HPF and nanophytosome-loaded HPF obtained from *J. polycarpus* fruit against breast cancer cells growth and apoptotic biomarkers. Our results showed that phenolic-rich fraction from *J. polycarpus* fruit, especially at a concentration of 50 mg TPC/kg/BW, significantly mitigates lipid peroxidation status and level of liver enzymes. While untreated mice revealed higher liver enzymes and MDA contents in their blood, mice supplemented with HPE, and nanophytosome-loaded HPF showed a significant decrease in the average of MDA and liver enzymes. Additionally, the expression of antioxidant enzymes, SOD and GPX, was significantly increased in the liver of mice after supplementation with nanophytosome-loaded HPF. These findings indicate that nanophytosome-loaded HPF has a protective effect on body organs by reducing oxidative damage and improving the antioxidant capacity. In a study, Mrid et al. (Ben Mrid et al. 2019) assessed the antioxidant properties of aqueous and methanol extracts of needles and berries of *J. oxycedrus* on breast cancer cell lines. They demonstrated that *J. oxycedrus* extract significantly improved the activity of SOD and GPX.

Moreover, the plant extract showed potent cytotoxic effects against breast cancer cell lines with no cytotoxicity towards normal cells. These results are closely consistent with the findings of our research. In our study, the extracts exhibited intense antioxidant activity.

Furthermore, nanophytosome-loaded HPF exhibited a cytotoxicity effect on breast cancer cells with no toxic effects. In our study, mice receiving nanophytosome-loaded HPF showed a higher average weight gain and food intake than the control group. These findings implicate the beneficial of nanophytosome-loaded HPF for the normal growth of body organs. To improve the antitumor activity of HPF, we loaded the HPF into a nanophytosome. Interestingly, our data revealed that nanophytosome-loaded HPF has a significant effect in inducing apoptosis in the tumor tissue. We found that the nanophytosome-loaded HPF not only decreased the expression of an anti-apoptotic biomarker bcl2, but also enhanced apoptotic biomarkers bax and caspase-3, in tumor tissue without any toxicity on normal cells. Besides, thus, this finding emphasizes that nanophytosome-loaded HPF can effectively target and inhibit tumor cells growth by inducing the apoptotic biomarkers. Some studies reported the antitumor effect of *J. polycarpus* fruit extracts on various cancer cell lines to support these findings. Benzina et al. (Benzina et al. 2015) considered the apoptotic properties of the flavonoid deoxypodophyllotoxin purified from the *J. communis* extract on MB231 breast cancer cells. They found that the extract induces cancer cell apoptosis by inducing the caspase-3 pathway.

Similarly, we found that *J. polycarpus* HPE, especially nanophytosome-loaded HPE, significantly promoted apoptosis via inducing the expression of the caspase-3 gene. More recently, Huang et al. (Huang et al. 2020) evaluated the antiproliferation and anti-metastasis efficacy of hinokiflavone compound extracted from *J. phoenicea* on human breast cancer cells. They reported that hinokiflavone significantly inhibited proliferation and induced apoptosis in breast cancer cells by modulating bax/bcl2 ratio. In addition, hinokiflavone remarkably inhibited migration and invasion of breast cancer cells. In our study, nanophytosome-loaded HPF significantly enhanced the expression of bax and reduced the bcl2 gene in tumor cells. These effects were comparable with the standard chemical tamoxifen drug.

Conclusion

In conclusion, we found that the HPF is very rich in phenolic metabolites. Furthermore, these extracts exhibited strong antioxidant capacity. Interestingly, HPF decreased lipid peroxidation and exhibited a protective effect on liver tissue by reducing the levels of liver-specific enzymes in a dose-dependent manner. To understand and improve the characteristic of the cytotoxicity effect of the HPF on human breast cancer cell lines, we incorporated these extracts of nanophytosome. Analysis of cytotoxic activity revealed a potential cytotoxic effect of nanophytosome-loaded HPF against breast tumor cells lines. However, the nanophytosome-loaded HPF appears to be not cytotoxic towards normal cells. We also found that nanophytosome-loaded HPF induced apoptosis of tumor cells through overexpression of bax and caspase-3 genes and down-regulation of bcl2. It appears that overproduction of reactive oxygen species, lipid peroxidation, and consequently induction of apoptosis pathways may be a potential action of nanophytosome-loaded HPF to inhibit tumor cell growth and proliferation. According to all the above results, it can be concluded that nanophytosome-loaded HPF could offer a beneficial and natural source of bioactive compounds that can be either used on the preventive side as used in the clinic without toxicity.

Material and methods

Plant material

Juniperus polycarpus fruits were collected from Chah chaheh, Razavi Khorasan Province, Iran, with the GPS location of 36.58608660658901, 60.37961020210671 on July 2020. The fruits of *Juniperus polycarpus* were identified and confirmed by the laboratory of plant taxonomy staff at the herbarium of Khorasan Razavi Agricultural and Natural Resources Research and Education Center, AREEO, Mashhad, Iran. The fruits were then rinsed and air-dried in a shady place at 25 °C for 10 days. Cholesterol, methanol, soybean phosphatidylcholine, and dichloromethane were bought from Merck Company (Darmstadt, Germany). All the other solvents and chemicals for this study were purchased from Sigma-Aldrich (Germany).

Extraction

Dried fruits were ground by a laboratory grinder to a fine powder and were extracted utilizing 80% methanol as solvent as described earlier by Crozier et al. (1997). Briefly, a dried sample of 0.5 g was weighed and placed into a 100-ml conical flask. Forty ml of 80% (v/v) methanol was added, followed by 10 ml of 6 M HCl. The combination was stirred using a magnetic stirrer. The mixture was placed in a round-bottom flask and attached to reflux and extracted for 2 h at 90 °C, after which the mixture was filtered utilizing Whatman No.1 filter paper (Whatman, England), and the filtrate was then taken to dryness with the aid of a vacuumed rotary evaporator (Buchi, Switzerland) at 60 °C.

Extract fractionation

The extract was fractionated using a separating funnel using hexane, chloroform, ethyl acetate, n-butanol, and water, as shown in Fig. 4. Each extraction was performed with 200 ml of fresh solvent, and the extraction for each solvent was carried out in triplicate. The obtained extract was filtered with Whatman No. 1 filter paper and concentrated

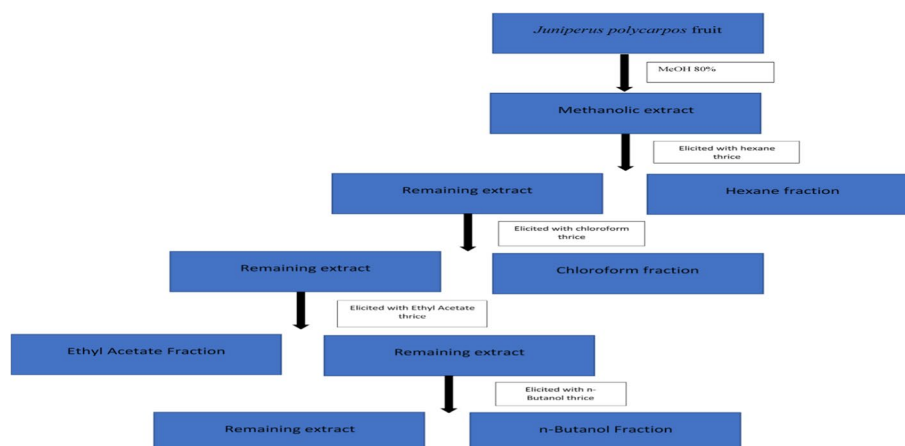


Fig. 4 Fractionation procedure

with the aid of a vacuum rotary evaporator (Buchi, Switzerland). The fractions were then dried in a freeze dryer and kept at $-20\text{ }^{\circ}\text{C}$ for total phenolic analysis. Each fraction's total phenolic compounds (TPC) evaluation was carried out by adding 0.1 ml of the extract, 2.5 ml of Folin–Ciocalteu reagent (1:10 v/v), and 2 ml of 7.5% sodium carbonate into a test tube covered with aluminum foil. The test tubes were vortexed, and the absorbance was measured at 765 nm (Oskoueian et al. 2020). The results were expressed as milligrams of gallic acid equivalents (GAE) per gram dry weight of each fraction. The fraction containing the highest phenolic content is named a phenolic-rich fraction (HPF). The test tubes were vortexed, and the absorbance was measured at 765 nm. The results were expressed as milligrams of gallic acid equivalents (GAE) per gram dry weight of each fraction. The fraction containing the highest phenolic content is named a phenolic-rich fraction (HPF).

Nanophytosomes preparation

Phytosomes can be produced by reacting phospholipids (1–3 mol) with an active substance (1 mol) in an aprotic solvent. In this study, nanophytosomes of HPF were produced in a ratio of 3:1 in ethyl acetate as an aprotic solvent. The complex was placed on a shaker overnight at a temperature of $55\text{--}60\text{ }^{\circ}\text{C}$ to dissolve completely. After removing the solvent using a freeze dryer, nanophytosomes were formed. The dynamic light scattering (DLS) technique was performed to ascertain particles' average size and stability (zeta potential). The measurements were examined three times by a Malvern Zetasizer Nano ZS (Malvern, UK). Furthermore, field emission scanning electron microscopy (FESEM) was applied to determine the size and shape of the nanophytosomes.

Phenolic profiling of nanophytosomes

To determine the phenolic compounds present in the nanophytosome, reversed-phase high-performance liquid chromatography (RP-HPLC) analysis was performed. The phenolic standards used in this study were gallic acid, syringic acid, vanillic acid, salicylic acid, caffeic acid, pyrogallol, catechin, cinnamic acid, ellagic acid, naringin, chrysin, and ferulic acid. The solvents consisted of deionized water (solvent A) and acetonitrile

(solvent B). The column was eluted and equilibrated by 85% solvent A and 15% solvent B for 20 min before injection. Then, the ratio of solvent B was increased to 85% after 60 min. After 5 min (at the 65th minute of running the experiment), the ratio of solvent B was reduced to 15%. This ratio was maintained for 70 min for the following analysis with a 1 ml/min flow rate. An analytical column (Intersil ODS-3 5 μ m 4.6 \times 150 mm GI Science Inc. USA) was used to detect phenolic compounds at 280 nm.

Toxicity assay

This assay was conducted to determine the toxicity of HPF using mice as an animal model. The 24 female Balb/c mice (at 4 weeks of age) were bought from the laboratory of the animal research center at Razi Vaccine and Serum Research Institute (Mashhad, Iran). Mice were adapted to the lab environment for one week and then randomly divided into 4 groups, including M1 (Control), M2 (25 mg/Kg/BW HPF); M3 (50 mg TPC/kg/BW HPF), and M4 (100 mg/kg/BW HPF). Mice were housed 3 per cage (30 \times 15 \times 15 cm) in a standard climate room (temperature of 22 \pm 2 $^{\circ}$ C, humidity 50% \pm 5%, and a 12:12 light/dark cycle) and had free access to food and tap water. 48 h after the final treatment (day 28), mice were anesthetized, and blood samples were directly collected from the abdominal aorta to measure blood tests analysis using a blood auto-analyzer (Hitachi 902, Japan). Liver, kidney, intestine, spleen tissues were isolated and fixed in 10% formalin for at least 48 h. Hematoxylin–eosin (H&E) staining was applied for morphological and histological examination of all tissues. The toxicity survey test was carried out in compliance with the OECD guideline No. 407. The mice trial in this research was approved by the ethical committee of Azad university of Mashhad and the laws, norms, and regulations dealing with international animal ethics (IR.IAU. MSHD.REC.1400.087).

Antiproliferative activity

To study the antiproliferative activity of HPF and phytosomes-loaded HPE, 32 female BALB/c mice (with an average age of 28 days and an average body weight of 19 g) were purchased from the laboratory animal research center at Razi Vaccine and Serum Research Institute (Mashhad, Iran). Upon 1 week of adaptation, the mice were randomly divided into four groups, animals in each group were housed 2 per cage (30 \times 15 \times 15 cm) in a standard climate room (temperature of 22 \pm 2 $^{\circ}$ C, humidity 50% \pm 5%, and a 12:12 light/dark cycle) and had free access to food and tap water. A cancerous cell line (TUBO breast cancer cell line) was obtained from Pasteur Institute (Tehran, Iran), and cultured in RPMI 1640 medium (Gibco, USA), supplemented with 10% inactivated fetal bovine serum (FBS) (Gibco, USA), 10% penicillin/streptomycin (100,000 U/L) (Gibco, USA). Cells were grown at 37 $^{\circ}$ C, under a 5% CO₂ atmosphere, and at 90% humidity for 24 h to reach ~80% confluency. Neubauer hemocytometer method was used to count cells. A total number of 5 \times 10⁵ TUBO breast cancer cells (in a volume of 50 μ l PBS buffer) were injected subcutaneously to the right flank of all animals. When the tumor size reached about 3 mm, the following treatments were applied for 28 days through daily gavage: control (T1); mice were receiving HPF (50 mg TPC/Kg/BW) (T2); mice were receiving nanophytosome-loaded HPF (50 mg TPC/Kg/BW) (T3), and mice receiving tamoxifen (0.4 mg/kg/BW similar dose to the clinical dose in humans) as an antiproliferative

drug (T4). The treatments were applied every day through oral gavage. All treatments received standard and balanced food pellets with free access to water. The corn oil was selected as a carrier of HPF and phytosomes. The control group has received corn oil devoid of HPF or phytosomes. Mice were monitored weekly by measuring tumor size using a digital caliper, and the tumor volume was also calculated by the following formula: $[(\text{length} \times \text{width} \times \text{height}) \times 0.52]$. The food intake and weight changes were determined weekly. According to the laws, norms, and regulations dealing with international animal ethics, all the procedures used in animal trials in this research were assessed and accepted by the ethical committee of the Islamic Azad University of Mashhad, Iran.

Samples collection

At the end of the experiment, mice were anesthetized, and blood samples were collected from the abdominal aorta to measure blood tests analysis. Liver, kidney, intestine, spleen, and tumor tissues were isolated for histological examinations and gene expression analysis. For histological examination, tissues were removed and fixed in 10% formalin for at least 48 h. Fragments were dehydrated in graded ethanol series, embedded in paraffin, and sectioned using an automatic microtome at 4–5 mm thickness. For histological processing, the sectioned tissues were stained with hematoxylin–eosin (H&E) and examined for morphological and histological parameters by light microscopy. For gene expression analysis, a fragment of tissues (50–100 mg) was isolated and immediately froze in the liquid nitrogen and kept at -80 for the gene expression analysis. The liver enzymes in the serum, such as alanine aminotransferase (ALT), alkaline phosphatase (ALP), and aspartate transaminase (AST), were determined using a blood auto-analyzer (Hitachi 902, Japan). The malondialdehyde (MDA) was determined as a marker of oxidative stress in the liver tissue (Shafaei et al. 2020). In brief, the liver tissue was homogenized, and 200 μl of lysate were mixed with 300 μl of water, 35 μl of BHT, 165 μl of Sodium dodecyl sulfate, and 2 ml of thiobarbituric acid, respectively. Upon heating (90 °C for 60 min), the solution was mixed with 2 ml of n-butanol and centrifuged at $3000 \times g$ for 5 min. The absorbance of the n-butanol part was determined at 523 nm, and the results were expressed as percentage malondialdehyde (MDA) changes relative to the control.

Gene expression analysis

The total RNA was extracted using AccuZol™ Total RNA Extraction Reagent kit (Bioneer Company, South Korea). The quantity and quality of extracted RNAs were evaluated using a Nanodrop spectrophotometer (Biotek Instruments). Electrophoresis, a fraction of each RNA sample on 1% denaturing agarose gel stained with ethidium bromide, was used to analyze the quality of RNAs. The cDNA synthesis kit (Fermentas, USA) containing RevertAid RT Reverse Transcription and Oligo dT primer was used for cDNA synthesis from RNA (5 μg) at 42° C for 1 h. A Rotor-Gene 6000 (CFX 96 Real-Time System) thermocycler in 36 cycles was applied for amplification. Each reaction included 10 μl 2X master mix, and 10 pmol primers, 1 μl template cDNA, and 8.2 μl ddH₂O in a total volume of 20 μl . Primer sequences of studied genes are shown in Table 11. The

Table 11 Primer sequences used in this study

Genes		Forward (5' to 3')	Reverse (5' to 3')
Mice	SOD	gagacctgggcaatgtgact	gtttactgcgcaatcccaat
	GPX	gtccaccgtgatgccttctcc	tctcctgatgccgaactgattgc
	β -actin	ggtcggtgtgaacggatttg	atgtaggccatgaggtccacc
Human	bax	ttgcttcagggttcatcca	ctccatgttactgtccagttcgt
	bcl2	catgtgtgtggagagcgtcaac	cagataggcaccagggtgat
	Caspase-3	ctggactgtggcattgagac	acaagcgactggatgaacc
	GAPDH	ccggatcgaccactacctgggcaac	gttccccactactggcccaggacca

mRNA expression levels of selected genes were normalized to the expression of either β -actin (for the mice genes) or GAPDH (for the human gene) as a house-keeping gene. The relative expression of studied genes was calculated using the $2^{-\Delta Ct}$ method (Livak and Schmittgen 2001).

Statistical analysis

All data were presented as means \pm SD. The one-way ANOVA: post hoc Tukey test was used to compare the mean of all data between groups. Data were analyzed using SPSS software (version 19). A $p < 0.05$ was considered significant.

Acknowledgements

The authors are grateful to the Islamic Azad University of Mashhad for the laboratory facilities.

Author contributions

SM: study design, experimental work, formal analysis and writing original draft; EK and EO: analysis, methodology, project administration, supervision, review, and editing of the original draft. All authors contributed equally to this work. All authors read and approved the final manuscript.

Funding

There has been no financial support for this work.

Availability of data and materials

The datasets applied during the current study are available on reasonable request.

Declarations

Ethics approval and consent to participate

This research does not contain any studies with human participants performed by any of the authors. All applicable international and national guidelines for the care and use of animals were followed. Research on experimental animals was carried out with the consent of the local ethics committee for animal experiments. All animal handling methods were accomplished as per the regulations of the Islamic Azad University of Mashhad, IRAN. Consent to participate-NA/Not applicable.

Consent to publication

Not applicable.

Competing interests

The authors declare that they have no competing interests.

Received: 3 December 2021 Accepted: 19 June 2022

Published online: 01 July 2022

References

Babazadeh A, Ghanbarzadeh B, Hamishehkar H (2016) Novel nanostructured lipid carriers as a promising food grade delivery system for rutin. *J Funct Foods* 26:167–175

- Babazadeh A, Ghanbarzadeh B, Hamishehkar H (2017) Formulation of food grade nanostructured lipid carrier (NLC) for potential applications in medicinal-functional foods. *J Drug Deliv Sci Technol* 39:50–58
- Babazadeh A, Zeinali M, Hamishehkar H (2018) Nano-phytosome: a developing platform for herbal anti-cancer agents in cancer therapy. *Curr Drug Target* 19:170–180
- Beatrice Magne NC, Zingue S, Winter E, Creczynski Pasa T, Michel T, Fernandez X, Njamen D, Clyne C (2015) Flavonoids, breast cancer chemopreventive and/or chemotherapeutic agents. *Curr Med Chem* 22:3434–3446
- Ben Mrid R, Bouchmaa N, Bouargal Y, Ramdan B, Karrouchi K, Kabach I, El Karbane M, Idir A, Ziad A, Nhiri M (2019) Phytochemical characterization, antioxidant and in vitro cytotoxic activity evaluation of *Juniperus oxycedrus* Subsp. *oxycedrus* needles and berries. *Molecules* 24:502
- Benzina S, Harquail J, Jean S, Beaugard AP, Colquhoun DC, Carroll M, Bos A, Gray AC, Robichaud AG (2015) Deoxypodophyllotoxin isolated from *Juniperus communis* induces apoptosis in breast cancer cells. *Anti-Cancer Agents in Med Chem* 15:79–88
- Crozier A, Lean ME, McDonald MS, Black C (1997) Quantitative analysis of the flavonoid content of commercial tomatoes, onions, lettuce, and celery. *J Agric Food Chem* 45:590–595
- Dumitrescu R, Cotarla I (2005) Understanding breast cancer risk-where do we stand in 2005? *J Cell Mol Med* 9:208–221
- Emami SA, Abedindo BF, Hassanzadeh-Khayyat M (2011) Antioxidant activity of the essential oils of different parts of *Juniperus excelsa* M. Bieb. subsp. *excelsa* and *J. excelsa* M. Bieb. subsp. *polycarpos* (K. Koch) Takhtajan (Cupressaceae). *Iran J Pharmaceutical Res* 10:799
- Enyew A, Asfaw Z, Kelbessa E, Nagappan R (2014) Ethnobotanical study of traditional medicinal plants in and around Fiche District, Central Ethiopia. *Curr Res J Biol Sci* 6:154–167
- Ghanbarzadeh B, Babazadeh A, Hamishehkar H (2016) Nano-phytosome as a potential food-grade delivery system. *Food Biosci* 15:126–135
- Hosseinihashemi S, Dadpour A, Lashgari A (2017) Antioxidant activity and chemical composition of *Juniperus excelsa* ssp *polycarpos* wood extracts. *Nat Prod Res* 31:681–685
- Huang W, Liu C, Liu F, Liu Z, Lai G, Yi J (2020) Hinokiflavone induces apoptosis and inhibits migration of breast cancer cells via EMT signalling pathway. *Cell Biochem Funct* 38:249–256
- Kulkarni GT (2011) Herbal drug delivery systems: an emerging area in herbal drug research. *J Chronother Drug Deliv* 2:113–119
- Livak KJ, Schmittgen TD (2001) Analysis of relative gene expression data using real-time quantitative PCR and the 2⁻ $\Delta\Delta$ CT method. *Methods* 25:402–408
- Moeini M, Ghasemi Y, Moeini S, Nejati M (2010) Analysis of antimicrobial, antifungal and antioxidant activities of *Juniperus excelsa* M. B. subsp. *Polycarpos* (K. Koch) Takhtajan essential oil. *Pharmacogn Res* 2:128
- Mohiti-Asli M, Ghanaatparast-Rashti M (2018) Comparing the effects of a combined phyto-genic feed additive with an individual essential oil of oregano on intestinal morphology and microflora in broilers. *J Appl Anim Res* 46:184–189
- Momenimovahed Z, Salehiniya H (2019) Epidemiological characteristics of and risk factors for breast cancer in the world. *Breast Cancer: Target Ther* 11:151
- Niazian M (2019) Application of genetics and biotechnology for improving medicinal plants. *Planta* 249:953–973
- Oskoueian E, Karimi E, Noura R, Ebrahimi M, Shafaei N, Karimi E (2020) Nanoliposomes encapsulation of enriched phenolic fraction from pistachio hulls and its antioxidant, anti-inflammatory, and anti-melanogenic activities. *J Microencapsul* 37:1–13
- Roleira FM, Tavares-da-Silva EJ, Varela CL, Costa SC, Silva T, Garrido J, Borges F (2015) Plant derived and dietary phenolic antioxidants: anticancer properties. *Food Chem* 183:235–258
- Selvakumar P, Badgeley A, Murphy P, Anwar H, Sharma U, Lawrence K, Lakshmikuttyamma A (2020) Flavonoids and other polyphenols act as epigenetic modifiers in breast cancer. *Nutrients* 12:761
- Shafaei N, Barkhordar SMA, Rahmani F, Nabi S, Idliki RB, Alimirzaei M, Karimi E, Oskoueian E (2020) Protective effects of anethum graveolens seed's oil nanoemulsion against cadmium-induced oxidative stress in mice. *Biol Trace Elem Res* 198(2):583–591
- Sindhumol P, Thomas M, Mohanachandran P (2010) Phytosomes: a novel dosage form for enhancement of bioavailability of botanicals and nutraceuticals. *Int J Pharm Pharm Sci* 2:10–14
- Topçu G, Erenler R, Çakmak O, Johansson CB, Çelik C, Chai H-B, Pezzuto JM (1999) Diterpenes from the berries of *Juniperus excelsa*. *Phytochemistry* 50:1195–1199
- Tutin T, Heywood V, Burges N, Moore D, Valentine D, Walters S, Webb D (1980) *Flora Europaea*. Univ Press, Cambridge
- Wangchuk P (2018) Therapeutic applications of natural products in herbal medicines, biodiscovery programs, and biomedicine. *J Biol Active Prod Nat* 8:1–20
- Weinberg OK, Marquez-Garban DC, Pietras RJ (2005) New approaches to reverse resistance to hormonal therapy in human breast cancer. *Drug Resist Updat* 8:219–233

Publisher's Note

Springer Nature remains neutral with regard to jurisdictional claims in published maps and institutional affiliations.